A MODERN SPACE SITUATIONAL AWARENESS SYSTEM FOR THE AGE OF BIG DATA

Thomas M. Jackson[1], H. Holland[1], G. Tuparev[1], H. Andreasyan[1], M. Steinbatz[2], W. Promper[3], D. Weinzinger[3], and E. Doeberl[3]

[1]*Tuparev AstroTech, 3 Sofiyski geroy Str., entr. 2 app. 28, Sofia 1612, Bulgaria. Email: tmjackson@tuparev.com*
[2]*University of Applied Sciences Upper Austria, Campus Wels, Stelzhamerstr. 23, 4600 Wels, Austria. Email: m.steinbatz@fh-wels.at*
[3]*ASA AstroSysteme Austria GmbH, Galgenau 19, 4212 Neumarkt im Mühlkreis, Austria. Email: d.weinzinger@astrosysteme.com*

ABSTRACT

We, Tuparev AstroTech and ASA AstroSysteme Austria, present our joint commercial Space Situational Awareness (SSA) network currently under development. Our planned system aims to cover current weaknesses in SSA systems, while achieving a balance between accuracy and efficiency. We aim to have ∼20 to 30 in-house and custom built SSA stations worldwide within this decade, designed and built for rapid deployment while reducing costs. Our software pipelines will optimise schedules using AI algorithms to account for a mixture of tracking and survey modes and observing conditions, run analysis in real-time, enable immediate follow-up of objects of interest, and efficiently store and allow easy access to petabytes worth of information on a bespoke archive. The data products we plan to offer will include tracking data messages and light curves in the initial stages, with orbital prediction and collision warning systems planned at later stages of development. Our system will also incorporate automatic systems to mine the data for scientific research purposes.

Keywords: Space Situational Awareness, Space Debris, Streak Detection, All-Sky Survey, Telescope Networks, Imaging, Artificial Intelligence, Data Archives.

1. INTRODUCTION

With the rapidly increasing amount of objects in orbit around the Earth, including active satellites, inactive satellites, and space debris, the need to track and classify such material using Space Situational Awareness (SSA) systems has never been greater. There are a number of SSA systems and networks currently in operation aiding in collision avoidance and clean-up efforts, including governmental, commercial, and research. Most of these networks, however, have deficiencies; in some cases, through their geographical or technical coverage, they may only target specific objects in certain orbits, or they are not set up to rapidly analyse the large amounts of data that will be possible in the coming years. These factors are key for an SSA system if it is to maximise its effectiveness.

On the technical side, current SSA networks use various hardware setups for the tracking and characterisation of satellites and space debris, such as Radar networks [e.g. 5, 1], laser ranging systems [e.g. 10, 9], and/or passive radio observations. Each of these hardware systems has their own advantages and disadvantages, though, meaning some organisations have turned to optical observations in the effort to detect new objects as well as to continuously track known objects.

A significant number of current optical networks use small- to mid-class telescopes, ranging from a 10cm mirror or aperture up to a maximum of 1 metre [e.g. 7, 16, 4], with a few specialised telescopes beyond this size [e.g. 14, 13]. Those networks using small-class telescopes can easily scale up their network, increasing their potential geographical coverage, however sometimes at the expense of depth. Additionally the homogeneity of larger networks may vary if components are not uniform, introducing biases or problems when trying to carry out analysis in an efficient way. On the other hand, larger class telescopes are expensive, usually reducing geographic and sky coverage due to cost limitations on the number of stations which can be built.

Similar to the hardware variations, there are various analytical techniques currently utilised in different optical SSA networks. The algorithms and techniques applied to the observational data in order to detect satellites or space debris range from segmentation [12], image shifting and stacking [15], template matching using either classical filters [8] or steerable filters [2], to image transforms [6, 3]. Each technique varies in its accuracy, computational complexity, run-time, contamination and noise levels, or the type of object it is best suited to detecting. Therefore, great care must be taken in selecting (or creating) a method if an SSA system is to be developed that is capable of accurate, real-time streak detection.

It follows, then, that the ideal SSA system for discovering new space debris and tracking known objects in the age of increasingly large amounts of data requires a number of characteristics: i) extensive geographical coverage, ii) effective and easy installation of the optical systems, iii) optimised algorithms for both observation scheduling and image analysis, and iv) efficient and extensive storage facilities and distribution methods. These are aspects we, Tuparev AstroTech and ASA AstroSysteme Austria (hereafter ASA), aim to address in our new SSA network that we are presenting here, which is designed for the age of big data - ASA Apollon[1]. Section 2 presents the hardware components of our SSA system, Section 3 outlines the software pipelines we are developing and utilising for the network, Section 4 presents the performance results of the first run of our software on synthetic data, and Section 5 outlines the data archive size and data products we intend to produce and store. As an extra point, Section 6 outlines our plans for mining the data produced by our SSA system for scientific purposes before we conclude in Section 7.

2. SSA STATIONS

In order to maximise the productivity of our SSA systems, the hardware underpinning our system needs to have a number of features: a simple and relatively homogeneous design, short construction time with rapid deployment, a fully integrated control system, and a wide field of view, to name a few. Such a system should also be fully automated, or robotised, for optimal performance.

2.1. Test Observatory

In order to implement such a system, we are initially utilising a test station to develop and refine our plans for a transportable and self-contained SSA station to be used in later stages. Located near the village of Sandl in Austria, the observatory is at an altitude of 880 metres and consists of a classical dome, an ASA H400 telescope coupled to an ASA direct drive mount, and a Moravian C5A-150M CMOS camera. Furthermore we have a Windows control computer, an Apple Mac mini for image and data analysis, and a standard weather station.

The ASA H400 has a 40cm primary mirror, with a Newtonian focus, yielding an f2.4 focal ratio. The ASA mount can slew at speeds of up to 50 degrees a second, has a pointing accuracy of a few arcseconds, and has sub-arcsecond tracking accuracy. In addition to this, the Moravian C5A-150M camera placed at the Newtonian focus of the H400 telescope has a 0.807 arcsec pixel scale, 151 megapixels and thereby a 7.6 square-degree Field of View (FoV). The camera also has a very good sensor linearity, relatively low dark current and read out noise, and can take subsequent exposures immediately after one another. The combination of a wide field of view provided by the fast focal ratio of the telescope and size of the camera, and the rapid slewing speeds and high tracking accuracy of the mount make this setup ideal for rapidly moving space debris in both survey and tracking modes.

The two computers contained in the observatory are setup to work like two halves of a brain: The Windows control computer uses in-house software programmed by ASA to control all equipment, including the dome, mount, camera etc. Communication with the observatory weather station also runs through this computer, which constantly measures the weather conditions, cloud cover etc. The connection of all observatory parts with the one computer means that the status of all devices can be monitored constantly and in scenarios where one device is not communicating or broken, or factors are present which could damage the systems (such as high winds or rainfall), the entire system automatically shuts down to preserve and protect the observatory. This is based on the architecture outlined in [11]. In addition to the control and monitoring, the schedules which are delivered from the central server to this computer will be updated in real-time to best exploit sky conditions and deal with the time constraints. Image data produced in standard FITS format by the telescope and camera are then delivered to the Mac mini. The Mac mini runs on Apple's M1 chip with 8GB of unified memory, an 8 core CPU, a 16 core GPU, a 16 core Neural Engine, and a 512GB solid-state storage capacity. The Mac mini runs all analysis operations on the imaging data delivered from the camera in the pipelines outlined in Section 3 and is responsible for the logging and temporary sorting and storage of all data.

2.2. Rapidly deployable SSA stations

Classical observatories, like our test observatory, can take months or years to complete from the initial design phases and site-searching through to the commencement of operations. To counteract these long timescales, we are currently aiming to develop a custom, in-house built observatory which can be rapidly deployed, an example of which can seen in Figure 1. These SSA stations will incorporate the capabilities of our optimised test observatory while minimising the construction times, reducing the installation times, and decreasing overall costs.

A standard shipping container provides the basis for these SSA stations, as seen in Figure 1, which removes the need to construct the usual (semi-)permanent enclosure at the observing site. The base container will be modified to include a raised dome, which will house at least one, potentially multiple, 0.4 to 1 metre-class ASA telescope(s). Additionally, each container will house a high-quality ASA mount, a Moravian C5-CMOS camera mounted to the telescope, and control and analysis computers as outlined in the previous section. Additional on-site data storage will be included in order to allow for extra capacity in case of emergencies, such as a loss of internet con-

[1] https://asa-apollon.com

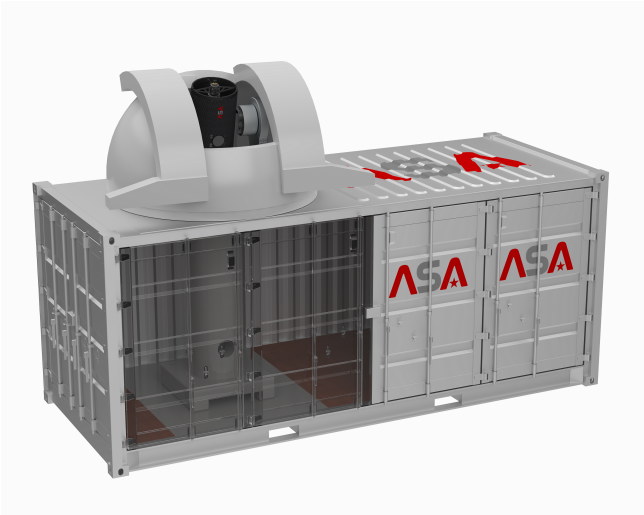

Figure 1: An example of the envisioned SSA stations currently under development. These will be built in-house by ASA AstroSysteme Austria and are designed to be reproducible, cut unnecessary costs without cuts in performance, and have rapid construction and deployment times.

nectivity, as well as a standard weather station and cloud monitor to protect the systems and optimise observations. Upon delivery to the respective observing site, each station will be easily and rapidly connected to electricity and internet, and once calibrated by our team over a few days, will be fully automated and integrated into our SSA network, significantly reducing deployment times compared to classical observatories.

3. SOFTWARE

In order to handle the significant amounts of data that will be generated by the telescope network and to maintain a high level of data accuracy, a number of pieces of software must be designed and developed to work in concert, including an optimised observation scheduler, a fast image reduction routine, a reliable streak detection algorithm, and an efficient way to transfer data to a central server. We outline how we are currently implementing the software for these processes throughout the following sub-sections.

3.1. Observation scheduling

An ideal observation schedule would be optimised to target specific objects when required by an observer, to better constrain orbital paths, while still surveying the sky otherwise in an attempt to detect previously unknown objects. There are, however, complicating factors (not least of which being the local weather and sky conditions) one must consider when building a scheduler and carrying out observations.

We initially generate a base schedule from the central control server to be sent to the windows control computer. Observations are scheduled to commence at nautical twilight and end at nautical dawn (operation times are likely to be revised as we improve the systems). We split the night sky into strips from the zenith to an approximate altitude of 50 degrees on the meridian, dividing each strip into fields as constrained by the camera field of view. For each field, we take 10 exposures before moving onto the next field down the meridian. At the end of each strip, the process is repeated, covering a new part of the night sky due to the Earth's rotation. This process will be transferred to a Right Ascension/Declination based system in later iterations of the scheduler when optimal schedules for multiple telescopes will be required. Each exposure will is likely to be 2 seconds so as to long enough to capture Geostationary Orbit (GEO) objects as streaks while still being short enough to capture Low Earth Orbit (LEO) objects moving rapidly across the field.

To maximise observing time, bias and flat-field images are scheduled to be taken during civil twilight. Due to the low noise nature of the CMOS cameras used for our systems, and the short exposure times used for survey mode objects, dark current noise is minimal. Constructed master bias and master flat-field frames are then used for the image calibration outlined in Section 3.2.

We are currently developing a constraint satisfaction algorithm to optimise the schedule both at the central control server before the start of each night and the on-site control computers in real-time. The constraint satisfaction algorithm treats the environmental constraints to the schedule assignments as if it were a Constraint Satisfaction Problem (CSP), which is heavily researched due to its ability to model and suggest solutions to complex, real-world situations. The initial schedule will be created by the central control server, while the on-site, real-time optimisation will weight factors such as distance of the field from the zenith, distance from the moon, any partial-sky cloud coverage, and distance from the previous field of observation to account for slewing times, and optimise the initial schedule between each set of observations.

Future iterations of the central scheduler will also include the ability to schedule specific tracking requests before the observation run starts, and the on-site scheduler will also include the ability to temporarily interrupt observations if a high priority target is requested at short notice, such as a gravitational wave event follow-up. Future versions over the next decade are also planned to account for two or more SSA stations at each observing site, one of which can be used for such tracking requests, following up detected streaks for more accurate orbital information, or for triangulation purposes to feed information into orbital models.

3.2. Image calibration and preparation

We firstly apply bias and flat-field corrections to the 10 raw images of each field (seen in the top panel of Fig-

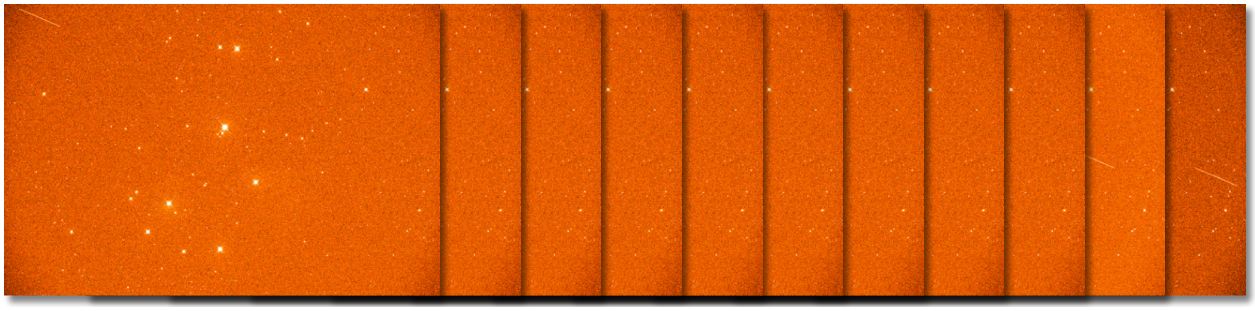

(a) 10 raw field images containing an artificially generated streak that have been fed into the pipeline for testing. The streak has a signal-to-noise ratio of 5 and stretches from the top left of the first image to the center right of the last.

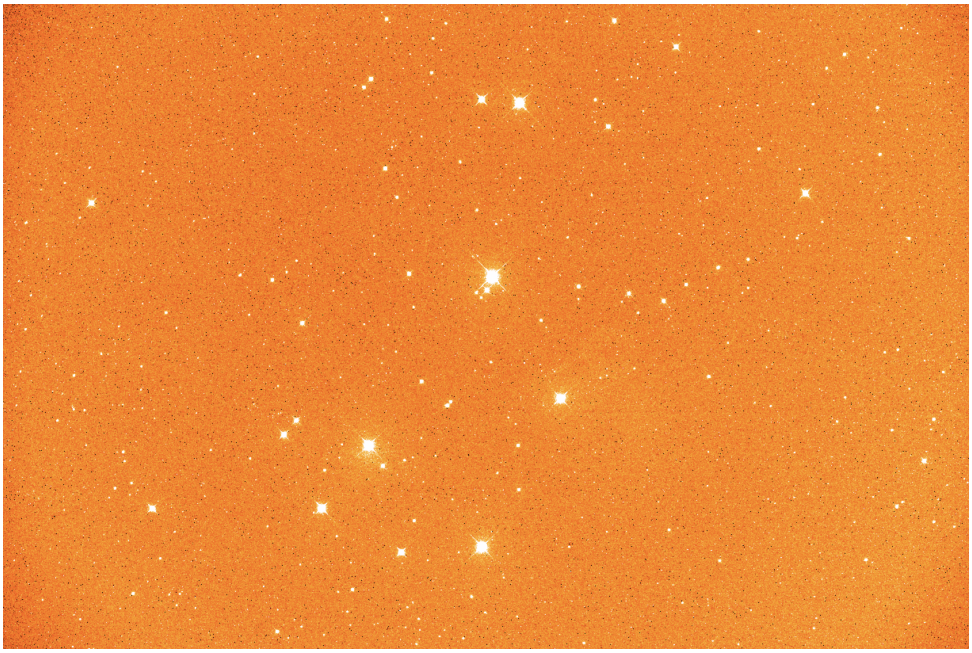

(b) The median science frame, created after the raw frame calibration by calculating the element-wise median of each calibrated frame. Median stacking has the effect of removing artefacts or moving objects in the data that isn't present in all frames.

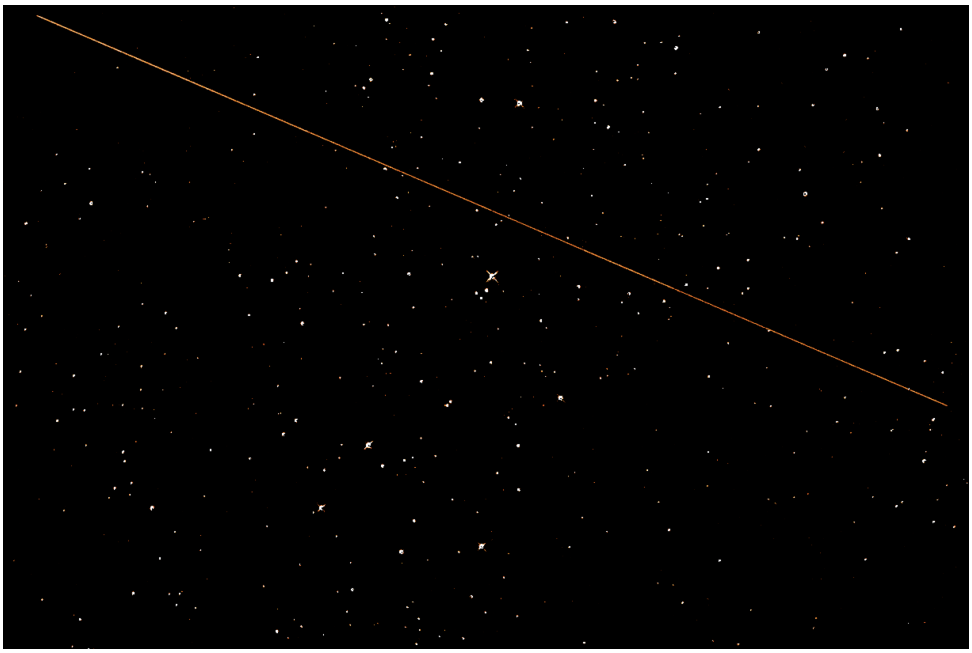

(c) The median-subtracted streak frame, created by subtracting the median science image in Figure 2b from each of the individual calibrated frames and summing the results. Most of the signal from the stationary background is subtracted away, leaving the transient streak.

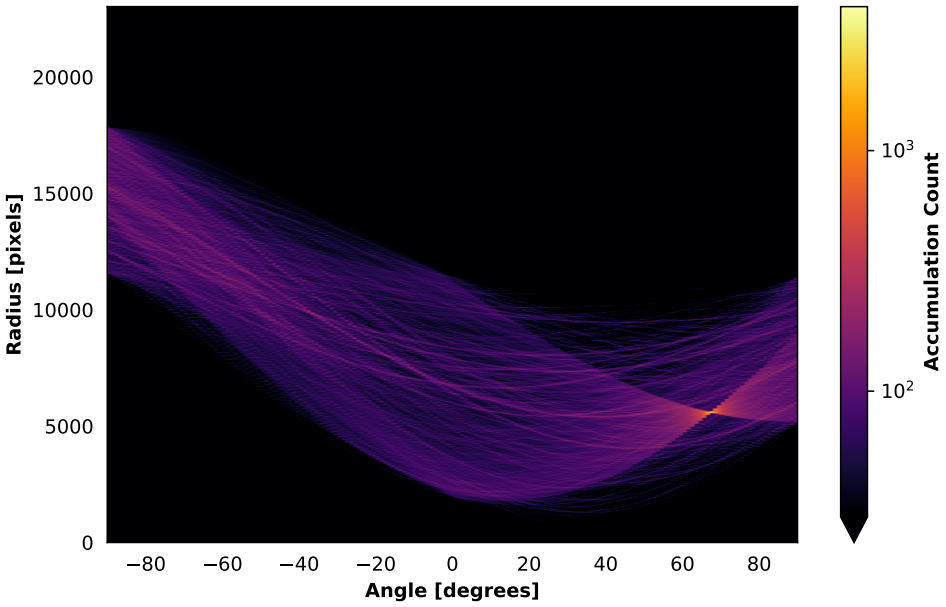

Figure 3: An example Hough space map, generated by the pipeline when applied to 10 night sky exposures containing an artificially injected streak. The imprint of the streak can be easily identified at an angle of $\sim$ 67 degrees and with a radius of $\sim$5500 pixels from the origin.

ure 2), resulting in 10 reduced and calibrated science-quality images. The 10 science images are then median-stacked, producing an "average" image of the field (seen in the central panel of Figure 2)), which is subtracted from each science image to remove the signal of background objects, such as stars or galaxies, producing "median subtracted images". This process leaves behind mainly image artefacts or streaks from moving objects, although some atmospheric effects are also captured. We then sum the median subtracted images together to increase the length, and thereby the signal, of any streaks present (bottom panel of Figure 2).

3.3. Streak detection

Sigma clipping is utilised to calculate the background noise of the summed image described in the previous section, and a cut in the S/N is made on the summed image. We then utilise the Hough transform, locating peaks in radius-angle space (also known as Hough space). An example of this can be seen in Figure 3. The radius and angle values of any probable streaks are then used as a secondary mask on the 10 science quality images, before we apply a density-based clustering algorithm to detect and assign any pixels belonging to any streak-like objects, with the movement of the streak(s) across the 10 images used to determine the direction of the object. From this entire process we generate a corresponding tracking data message (TDM) for any streak that is detected, as well as calibrated science images of the field. We note that we are also currently trialing streak detection techniques such as Radon transforms or Machine-Learning algorithms to compare performance in efficiency and accuracy.

4. PIPELINE PERFORMANCE

4.1. Accuracy

We artificially injected 100 different streaks into 10 raw exposures of the star cluster M45, taken using the test observatory. Each streak was injected with signal-to-noise ratios of 10, 5, 3, 2, 1.5, 1.0, and 0.5, resulting in 700 fields, and 7000 images. The pipeline streak detection results are presented in the top panel of Figure 4, and show a very high (85-90%) detection percentage for streaks with a signal-to-noise ratio ≥ 2. We also see in the bottom panel of Figure 4 that of the 10 field frames, each with a streak segment in them, the pipeline detects at least 9 of those 10 in greater than 75% of the test fields (the box plots indicate the 25^{th} and 75^{th} percentiles), given that the streak's signal-to-noise ratio is greater than or equal to 2. Higher numbers of these segments detected means greater accuracy when determining the position and motion of the satellites or space debris (see Sections 5.2 and 6).

We expect small errors when determining streak endpoints during the detection and extraction process. These errors are characterised in Figure 5, where we have compared the difference in the original x and y pixel coordinates given to the artificially injected streak to the coordinates found by the pipeline. The box plots indicate the median and the 25^{th} and 75^{th} percentiles. We can see that irrespective of the signal-to-noise ratio of the streak, the majority of endpoints are correctly identified to within 5 pixels of their true location, translating to 4 arcseconds. We also notice some small systematic trends, such as the

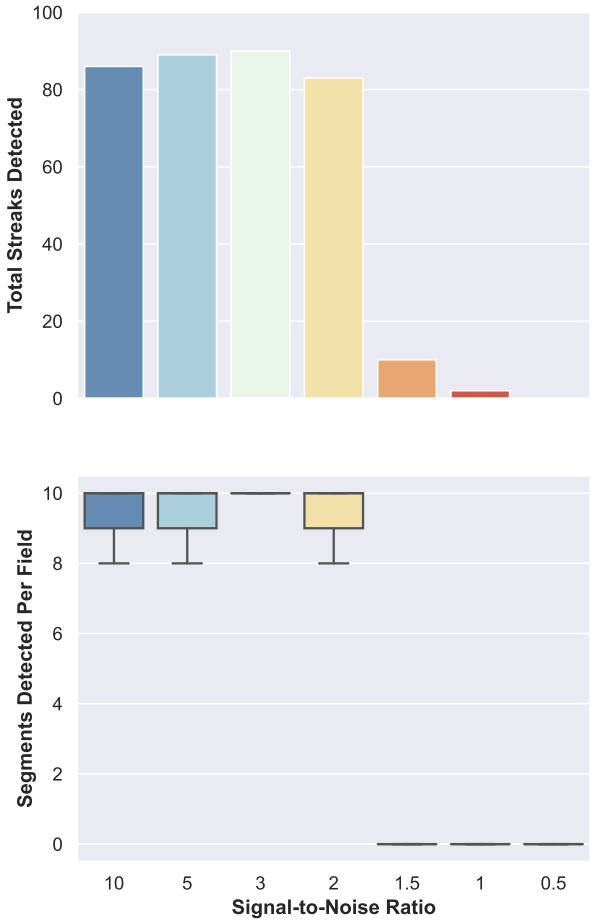

Figure 4: Top panel: The detection fraction of 100 artificially injected streaks into a 10 image data set as a function of signal-to-noise. Bottom panel: The number of streak segments per field detected by the clustering algorithm as a function of the signal-to-noise for the 100 artificially injected streaks. The initial pipeline performance is relatively high for streaks with a signal-to-noise of 2 or above.

asymmetric shifting of the value of y_1 and y_2 at high signal to noise, which is currently being investigated. The length of the whiskers of each distribution have lengths of either 1.5x the inter-quartile range or they extend to the farthest point within that distance, whichever is shorter.

4.2. Efficiency

In order for the processing of a field to begin immediately after its exposures are complete, it is important for the pipeline's execution time to be as close to the total exposure time as possible. As discussed in Section 3.1, each field will be imaged with 10 consecutive 2-second exposures. Allowing for 5 seconds on the slewing time and other overheads of the telescope, that yields a total effective field time of 25 seconds, setting the goal for the pipeline's run time. As of the time of writing, if an field

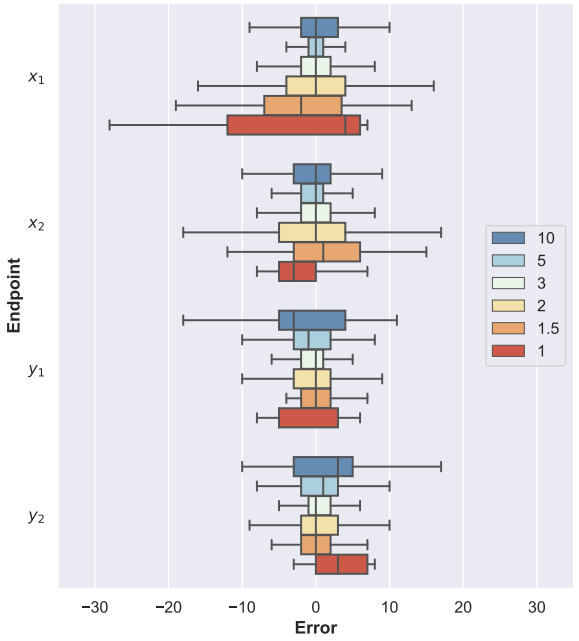

Figure 5: The distribution of differences between the detected streak endpoints (x_1, x_2, y_1, y_2) and the true values for a dataset of 100 artificially injected streaks, each injected into 10 raw images. The distributions are grouped by endpoint and colored according to the signal-to-noise ratio of the injected streak, with the median, $25^{\rm th}$ and $75^{\rm th}$ percentiles indicated by the boxes. Outliers on this plot have been removed for visual clarity. The length of the whiskers of have lengths of either $1.5 \times IQR$ or they extend to the farthest point within that distance, whichever is shorter.

has a streak with a signal-to-noise ratio $\geq$3, the likelihood that it will be processed in 25 seconds or less is $P \approx 0.8$ with the current hardware. We anticipate this likelihood to increase over the coming months as we explore more efficient and optimal methods of streak extraction. For the same reason, we also anticipate this likelihood to hold for lower signal-to-noise ratios—potentially as low as S/N = 1.0 or S/N = 0.5.

5. DATA ARCHIVE AND PRODUCTS

A key part of our SSA network is the data archive. The data archive acts as the central point for all data, including the push and pull systems to deliver data.

5.1. Expected data sizes and transfer

The calibrated science quality images, although an intermediate step in the pipeline, are a useful data source on their own. Such images can be used to calibrate or check existing measurements, cross-check methods, or for scientific research. The 10 calibrated frames of each field are saved as 10 image extensions of a single FITS file. With each pixel stored as a 32-bit floating point number, and 151 Megapixels per image, each uncompressed image takes approximately 604 megabytes of storage space, thereby meaning that each 10-image FITS file will require 6 gigabytes of storage space.

This image is saved to a monitored folder on the Mac mini, and when this folder's contents change, the new contents are automatically added to a queue to be uploaded to the central server. Since the file sizes are rather large, the science images will firstly be compressed using a standard FITs compression algorithm before beinf scheduled for uploading. As TDMs will receive priority over science images, and because we expect data to be generated faster than all files can be uploaded, the upload process is likely to continue into the daytime, when observations have ceased.

We also expect a single observatory to be able to observe over 1000 individual fields per night, which results in approximately 1 to 2 terabytes of data collected per observatory, per night at maximum capacity. Taking into account redundancy, we expect upper limits of hundreds of petabytes of data per year when the full network is operational. This therefore requires a bespoke petabyte-size data archive, currently in the early design stages.

Once the data products from our pipeline are successfully uploaded to the central server, they will be made available through two different systems: push and pull. In push delivery, clients will be able to agree to an automatic delivery of data every 12 or 24 hours (agreements can be made for longer or shorter delivery intervals), which will be delivered via SFTP protocol. In the pull delivery option, clients will be able to access a portion of the central server and the data products contained within through an interface. The data types presented in the following sub-sections will be available through both options upon agreement with each individual client.

5.2. Data Products

We will offer TDMs in both of the standard XML and KVN formats, conforming to the standards of the Consultative Committee for Space Data Systems[2] (CCSDS). These TDMs will contain all positional information we can provide. Additionally, we will also extract the photometry of any detected streak objects, calibrated and measured in white-band magnitudes, to be included in the TDMs. These magnitudes will provide information on the light curves of objects, which we intend to include in future versions in the form of a library of light curves of known or identified objects.

Some clients may wish to run their own algorithms on our data, from calibrating their own measurements, to cross-matching results from different methods, through to completely independent measurements. Hence, we will additionally enable access to the calibrated imaging data. These will be stored in the format described above, in standard FITS format, with a top level header with appropriate metadata (such as the field identifier and number of streaks), 10 lower level image units with the 10 calibrated science frames and, if any streaks are found, a 11th binary table extension containing the streak information.

We aim to make the images available for 3 to 6 months before deletion, which we believe is a suitable time-frame for any client to run their own algorithms or measurements on, without exceeding the expected storage capacity limits of our archive. TDMs will be stored for longer timescales, in the case that clients wish to compare previous measurements or run longer term modelling.

6. SCIENTIFIC POTENTIAL

A data set with the size and scope as that which will be produced by our SSA system has a significant scientific potential. The envisioned all-sky coverage, relative homogeneity of the network, and regularity of observations are all advantageous. Similarly advantageous is that the project is a commercial enterprise, meaning the network has the potential to operate for multiple decades, providing longer-term observations than nearly every system currently available. This allows us to concentrate on two particular areas: long-term photometric catalogues and all-sky imaging.

By identifying stars and galaxies within our median stacked science images of each field of observation, we can measure the fluxes of thousands to millions of objects per night. Long-term photometric measurements over decades can be useful for investigating astronomical objects such as long-term variable stars and certain rare types of galaxies such as so-called "changing look" Active Galactic Nuclei. Rare objects such as these currently lack measurements over extended timescales.

On the other hand, co-adding multiple images can serve to maximise the depth of the imaging data. This technique has been applied to a number of scientific surveys in recent years and can be used for galaxy evolution studies such as the characterisation of low surface brightness features, galaxy structure studies or to discover new, faint galaxies. We hope that by continually stacking our imaging data over a few years, we can aim to create the deepest optical all-sky image ever taken. Sky conditions, varying pixels scales of different cameras due to upgrades, astrometry differences or uncertainties etc. will also need to be accounted for carefully though, in both the co-addition

[2] https://public.ccsds.org/default.aspx

and photometry.

7. SUMMARY

In summary, we, Tuparev Astrotech and ASA AstroSysteme Austria have presented an overview of our planned Space Situational Awareness (SSA) network, currently in the early stages of development. Our SSA system will consist of ∼20 to 30 custom-built stations, deployed worldwide over the coming decade, covering a greater geographical and celestial area than most currently available commercial systems.

The hardware components and systems are currently being developed at a test observatory, with rapidly deployable stations expected soon. Our entire system will be fully autonomous, with automatically optimised schedules from the central server and robotic observations carried out by the SSA stations. On-site analysis computers will rapidly calibrate the imaging data and extract satellite and space debris via streak detection by use of the Hough transform and clustering algorithms.

The data produced from this analysis will include TDMs and science images with the aim of offering orbital estimations and light curves for satellites and space debris in future versions. The data itself will be transferred to and stored on a bespoke petabyte-scale central data archive, and delivered to clients through push and/or pull systems according to their individual needs.

ACKNOWLEDGMENTS

The authors would like to thank Moravian Instruments Inc. for their support, discussions and advice about the imaging devices used in this project.

T. M. J. would also like to thank Dr James Osbourne at Durham University for his wider discussions on the topic of Space Situational Awareness systems.

REFERENCES

1. Apa R., Bonaccorsi S., Piravano L., Armellin R. (2021). *Combined Optical and Radar Measurements for Orbit Determination in LEO.* 8th European Conference on Space Debris.

2. Cvrcek V., Radim S. (2021). *On Fast Matched Filter for Streak Detection and Ranking.* 8th European Conference on Space Debris.

3. Hickson P. (2018). *A fast algorithm for the detection of faint orbital debris tracks in optical images.* Advances in Space Research, 62, 3078

4. Jilete B., Mancas A., Flohrer T., Krag H. (2019). *Optical Observations in ESA's SSA Programme.* Revista Mexicana de Astronomia y Astrofisica Conference Series. pp 139–143

5. Murray J., Kennedy T., Miller R., Matney M. (2021). *Radar Observations from the Haystack Ultrawideband Satellite Imaging Radar in 2019.* 8th European Conference on Space Debris.

6. Nir G., Zackay B., Ofek E. O. (2018). *Optimal and Efficient Streak Detection in Astronomical Images.* Astron. J., 156, 229

7. Park J., Yim H., Choi Y., Hyun J., Moon H., Park Y., Bae Y., Park S. (2017). *OWL-Net : A Global network of robotic telescopes dedicated to SSA observation.* 7th European Conference on Space Debris.

8. Schildknecht T., Schild K., Vannanti A. (2015). *Streak Detection Algorithm for Space Debris Detection on Optical Images.* Advanced Maui Optical and Space Surveillance Technologies Conference 2015. p. 36

9. Steindorfer M. A., Kirchner G., Koidl F., Wang P., Antón A., Fernández Sánchez J., Merz K. (2017). *Stare and chase of space debris targets using real-time derived pointing data.* Advances in Space Research, 60, 1201.

10. Steindorfer M., Wang P., Kirchner G., Koidl F. (2021). *The future of space debris laser ranging - Towards high precision MHz daylight space debris laser ranging?* 8th European Conference on Space Debris.

11. Tuparev G., Andreasyan H. R., Jackson T. M. (2022). *Robotising Existing Astronomical Observatories* Communications of BAO, Vol. 69, Issue2, 2022, pp.302-307.

12. Virtanen J., Poikonen J., Säntti T., Komulainen T., Torppa J., Granvik M., Muinonen K., Pentikäinen H., Martikainen J., Näränen J., Lehti J., Flohrer T. (2016). *Streak detection and analysis pipeline for space-debris optical images.* Advances in Space Research, 57, 1607

13. Wagner G., Schramm F., Riede W., Dekorsy T., Döberl E., Weinzinger D. (2021). *Platform for Future Optical Space Surveillane Technology: DLR's 1.75m Optical Telescope.* 8th European Conference on Space Debris.

14. Woods D., Shah R., Johnson J., Szabo A., Pearce E., Lambour R., Faccenda W. (2012). *The Space Surveillance Telescope: Focus and Alignment of a Three Mirror Telescope.* Advanced Maui Optical and Space Surveillance Technologies Conference. p. 29

15. Yanagisawa T., Nakajima A., Kimura T. (2005). *"The stacking method": The technique to detect small size of GEO debris.* Science and Technology Series, 109, 29

16. Zhang C., Ping Y., Zhao C. (2018). *Wide field survey, telescope system, survey strategy.* The Advanced Maui Optical and Space Surveillance Technologies Conference 2018.